

PAPER • OPEN ACCESS

An experimental investigation on the effects of cylindrical rods in a draft tube at part load operation in down-scale turbine

To cite this article: S Shiraghaee *et al* 2022 *IOP Conf. Ser.: Earth Environ. Sci.* **1079** 012007

View the [article online](#) for updates and enhancements.

You may also like

- [Investigation of the Plunging Pressure Pulsation in a Swirling Flow with Precessing Vortex Rope in a Straight Diffuser](#)
S Muntean, C Tnas, A I Bosioc et al.
- [Experimental Investigation of the Unsteady Pressure Field in Decelerated Swirling Flow with 74° Sharp Heel Elbow](#)
D C Mo, S Muntean, A I Bosioc et al.
- [Vortex rope interaction with radially protruded solid bodies in an axial turbine: a numerical study](#)
H Holmström, J Sundström and M J Cervantes



ECS
The
Electrochemical
Society
Advancing solid state &
electrochemical science & technology

DISCOVER
how sustainability
intersects with
electrochemistry & solid
state science research

An experimental investigation on the effects of cylindrical rods in a draft tube at part load operation in down-scale turbine

S SHIRAGHAEI¹, J SUNDSTRÖM¹, M RAISEE², M J CERVANTES¹

¹ Department of Engineering Sciences and Mathematics, Luleå University of Technology, Luleå, Sweden

² Hydraulic Machinery Research Institute, School of Mechanical Engineering, College of Engineering, University of Tehran, Tehran, Iran

shahab.shiraghaee@ltu.se

Abstract. The present work examines the effects of the radial protrusion of four cylindrical rods at different lengths within the flow field of a down-scaled turbine draft tube under part-load operating conditions. Four rods were placed on the same plane 90 degrees apart. The protrusion length was varied from zero to approximately 90 % of the draft tube radius. Time-resolved pressure measurements were performed to quantify the effect of the rod protrusion, using two pressure sensors at the same vertical level 180 degrees apart. Such sensor configuration enabled the decomposition of the signals into rotating and plunging components of the rotating vortex rope (RVR). The results show that different levels of mitigation are achieved for the rotating and plunging components depending on the protrusion length. The effects on the plunging component differ from the ones on the rotating component. The RVR plunging pressure pulsations slightly increase with the initial rod protrusion and then significantly drop after a certain length. On the contrary, the rotating component of the pressure pulsation amplitudes immediately decreases with the onset of rod protrusion. However, an optimum length is obtained in both cases where the highest mitigation occurs before reaching the maximum protrusion. This observation falls in line with the previous investigations conducted for oscillatory rod protrusions, further approving the point that a closed-loop controller should accompany the mitigation technique to achieve optimum mitigation.

Keywords: Hydraulic turbine, stationary rod protrusion, rotating vortex rope, draft tube, pressure pulsation.

1. Introduction

The Part-load operation of hydraulic turbines is becoming more common today to regulate the electricity production of intermittent energy sources [1]. The deceleration of swirl inside the draft tube of hydraulic turbines causes vortex breakdown in this operating condition, leading to a rotating vortex rope (RVR). The formation of the RVR inside the draft tube induces pressure fluctuations that may travel through the entire conduit [2]. RVR pressure oscillations appear in the form of a rotating component as well as a plunging one. RVR rotating mode originates from vortex breakdown inside the draft tube; thus, it is a local phenomenon that dominates in the draft tube [2, 3]. The contribution of the



rotating mode to the overall RVR pressure fluctuations is more significant inside the draft tube compared to the plunging mode [4, 5]. However, since the plunging mode appears due to the existence of the elbow, the consequent standing waves cause pressure fluctuations that travel over the entire conduit [2]. The plunging mode is also more likely to resonate with the system given its synchronous nature [6]. These fluctuations cause a decrease in efficiency and jeopardize the structural health of the turbine by imposing cyclic loads on runner blades as well as turbine stationary parts, hence, increasing the possibility of wear, tear, and resonance [7]. Ideally, a mitigation technique should address both components. However, the immediate vicinity of the discharge section to the turbine's rotating parts indicates that the high amplitude of the RVR rotating mode is more important to be avoided.

Various methods have been proposed for the mitigation of RVR. These techniques include flow injection inside the draft tube as well as alterations of the draft tube geometry. Water and air injection have been investigated at the tip of the runner crown and the walls of the draft tube [8-13]. Bosic et al. [6] studied water injection from the runner crown into the vortex region. They managed to reduce RVR pressure fluctuations by an order of magnitude injecting 11.5% of the inlet flowrate. Holmström et al. [14] numerically investigated the azimuthal injection of pulsating momentum from four nozzles on the draft tube wall. Their results indicated significant mitigation of the rotating component and overall amplitude of the RVR pressure pulsations achieved for a jet flow ratio of approximately 5%. Nishi et al. [15] examined the effect of fins inside the draft tube. They observed a decrease in pressure fluctuation amplitudes along with an increase in the RVR-related frequency. Zhou et al. [16] investigated baffles mounted on the draft tube wall. They managed to mitigate the pulsations, which they attributed to the increase of flow axial velocity and decrease of the tangential velocity as a result of baffles. They also observed a slight rise in the RVR frequency that they considered negligible. Tanasa et al. [17] employed a diaphragm mechanism at the outlet of a conical diffuser. The RVR rotating component amplitude was significantly reduced by closing the diaphragm while the plunging component slightly increased. They also managed to improve the pressure recovery and change the structure of the RVR from a helical vortex shape into a bubble shape. Shiraghaee et al. [18] studied the effect of oscillating rod protrusions inside the draft tube. Their results displayed significant mitigation of the rotating component along with an increase of the plunging component. They attributed the mitigating effects to the interaction of the rods with the tangential flow region, the introduction of momentum into the stagnant region, and the interaction of the rods with the stagnant region interface. Joy et al. [19] studied the effects of adjustable guide vanes inside the draft tube. By re-directing the flow at part-load to the angles associated with the BEP condition, they achieved substantial RVR mitigation levels while the pressure recovery slightly increased.

The studies carried out have explored different ways to mitigate the RVR. However, no universal solution has been achieved yet. Nonetheless, given the variable nature of the RVR depending on the operating condition, the need for a simple yet robust solution that can adapt to different operating conditions is necessary. Adjustable geometries are suitable alternatives in this regard.

The current paper aims to investigate the radial insertion of four cylindrical rods inside the draft tube at part-load operating conditions. All the cylindrical rods are located on the same horizontal plane, separated by 90 degrees. Different lengths of rod protrusion are examined, and their effects on the RVR are analyzed based on the time-resolved pressure data collected on the draft tube walls.

2. Experimental apparatus

The experiments in the current study were performed at Luleå University of Technology, Sweden, on a scaled-down model of the U9 Kaplan turbine with a scaling ratio of 98/1550. The runner, draft tube, elbow bend, and diffuser are geometrically similar to the prototype. However, the spiral casing and distributor are not homologous to the prototype. This model contains 10 guide vanes that lead the flow to a runner with a diameter of $D_T = 98$ mm. The runner was 3D printed using a glass-filled rigid 4000 resin; thus, the blade angle was fixed at an angle coinciding with that extensively studied by Amiri et al. [2, 4] in a 1:3.1 model of the U9 prototype. Four LinMot ps01-23x80 linear motors were used to

insert the four rods with a diameter of $D_R = 10$ mm into the draft tube. For this purpose, four holes were drilled on the sides of the draft tube at an axial position of 4 mm downstream of the runner hub. These holes were separated by 90 degrees, covering the entire draft tube's periphery. Figure 1 displays schematics of the draft tube, spiral casing, linear motors, and the pressure sensors.

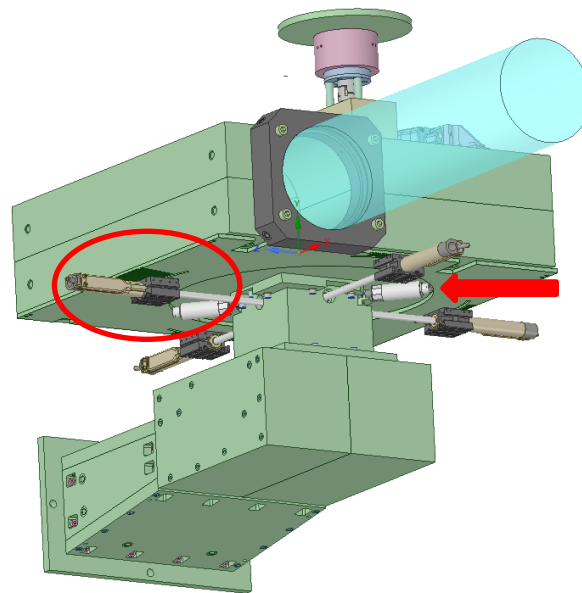


Figure 1. Schematic of the spiral casing, draft tube, position of the linear motors (marked in red circle), and the relative position of the pressure sensors (marked with red arrow) used in these experiments.

Two UNIK 5000 pressure sensors with a range of ± 7 kPa were mounted 180 degrees apart at an axial location coinciding with the bottom of the runner hub. The 180 degrees spatial separation of the sensors at the same horizontal level allowed the decomposition of the pressure signals into rotating and plunging components of the RVR. A Honeywell FDW differential pressure sensor with a range of ± 0.5 bar measured the pressure drop across the turbine to calculate the turbine head, H_T . The signals were recorded at a sampling frequency of 2 kHz using a National Instruments PXI-4472 ADC data acquisition system with a resolution of 24 bits. An optical sensor and a Krohne optiflux electromagnetic flowmeter measured the runner rotation frequency, f_n , and the flow rate, Q_T , respectively. A Magbrakesystems MBL-3.75 magnetic brake was installed parallel with the turbine shaft to control the turbine angular velocity, N_T . In its original configuration, the rotating system had small inertia, thus making the turbine prone to variations in the angular velocity. A 2.5 kg flywheel with a 200 mm diameter was installed on top of the magnetic brake to increase the polar moment of inertia by a factor of approximately 40 inducing better controllability.

3. Experimental approach

Several measurements were performed to provide a hill chart based on the values of $Q_{11} = Q_T / D_T^2 H_T^{1/2}$ and $N_{11} = N_T D_T / H_T^{1/2}$ with the corresponding pressure fluctuation amplitudes. The pressure signals collected over 30 s were decomposed according to equations (1) and (2):

$$P_r = \frac{P_1 - P_2}{2} \quad (1)$$

$$P_p = \frac{P_1 + P_2}{2} \quad (2)$$

where P_1 , P_2 , P_r , and P_p are the signal collected from pressure sensor number one, pressure sensor number two, the rotating and plunging components of pressure oscillations, respectively. Then, Fast Fourier transform (FFT) was conducted on the decomposed pressure signals to compare RVR fluctuation levels. The FFT values corresponding to the rotating and plunging component of the RVR were extracted and used to create a map of the RVR-related amplitudes based on the operating condition. Figure 2 presents the RVR amplitude maps of the rotating and plunging components.

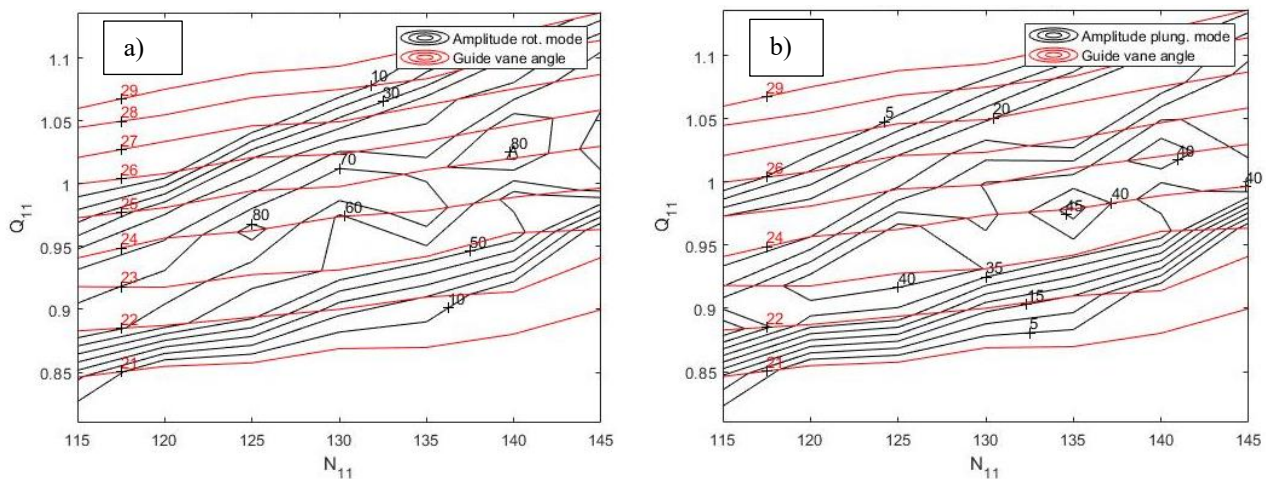


Figure 2. The RVR amplitude mappings prepared for the model test rig used in the present experiments. *a)* map of the rotating component amplitudes, *b)* map of the plunging component amplitudes. The amplitude of the pressure is in Pa.

The objective was to avoid both deep part-load and high part-load conditions characterized by high and low values of the rotating component amplitudes, respectively. Thus, a guide vane opening of 26° was chosen with $N_{11} = 125$ rpm and $Q_{11} = 1$ m³/s. Part-load RVR at this operating condition has smaller rotating component amplitude compared to smaller guide vane openings. However, the rotating component is dominant over the plunging component, and its value is still significant and more stable compared to higher guide vane openings. At this operating point, the runner passing frequency is $f_n = 12.5$ Hz and the RVR frequency is $f_{RVR} = 2.25$ Hz. The ratio of these frequencies is similar to the previous experiment on the corresponding model and prototype [2, 4, 20-22].

The measurements involving rod protrusion were run over 60 s in two sequences. In the initial sequence of 30 s, the flow was unperturbed without any rods inserted. Then, the rods were inserted at the desired length, and the measurement ran for another 30 s. Each case was repeated five times in these experiments to ensure the measurement's repeatability, and the standard deviation obtained was below 10%.

4. Results

Figure 3 shows the effect of rod protrusion length on the RVR rotating and plunging component average amplitudes. The protrusion length is presented in the form of a nondimensionalized length defined as follows:

$$L^* = \frac{L}{R_T} \quad (3)$$

where L is the length of protrusion and R_T is the radius of turbine runner.

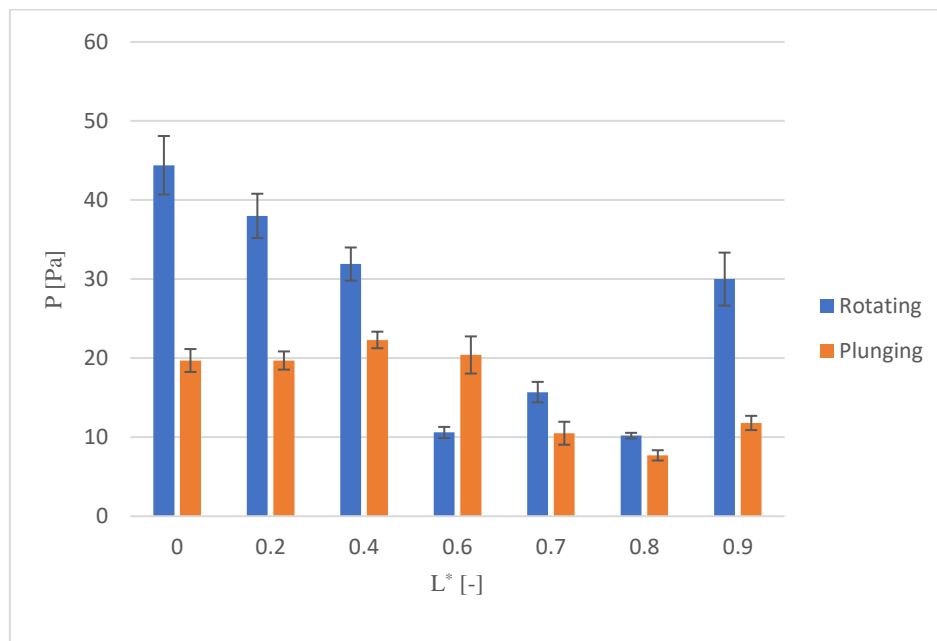


Figure 3. Average values of the rotating and plunging mode amplitudes for different protrusion lengths. The error bars represent standard error.

At zero rod protrusion, the rotating component dominates over the plunging component at this operating point, in agreement with the observations of Amiri et al. [4] regarding the pressure amplitudes of the RVR inside the draft tube of a 1:3.1 model of the U9 turbine. The strong local swirl of the flow at the position of the sensors (near the runner) gives rise to a stronger rotating component compared to the plunging mode, which originates from the bottom of the draft tube.

The rotating component decreases with the increase of protrusion length up to $L^*=0.6$. The decrease of the rotating component continues until the plunging component becomes dominant over the rotating component at $L^*=0.6$. By further increasing the protrusion length to $L^*=0.7$, the mitigation level drops from 76% at $L^*=0.6$ to 67%. Then, the highest mitigation of the rotating component is achieved at $L^*=0.8$ with 77%. Finally, the mitigation of the rotating component significantly decreases as the protrusion length is increased to $L^*=0.9$.

The plunging component of the RVR slightly increases with protrusion of the rods up to $L^*=0.6$. As aforementioned, the rotating component at this protrusion length has already decreased substantially while the plunging mode is still rather unaffected. The mitigation of the rotating component takes place through the deceleration of the swirl near the walls. However, at small protrusion lengths, the axial momentum in the center of the draft tube increases [16]. This results in both shrinkage of the stagnant region and a slight amplification of the plunging mode. Hence, further protrusion of the solid bodies is required to effectively disrupt the axial motion of the instability that is the plunging mode of the RVR. A considerable drop of the plunging mode amplitude takes place at $L^*=0.7$ and continues until $L^*=0.8$ where maximum plunging mode mitigation is achieved with 61%. Further protrusion of the rods to $L^*=0.9$ only decreases the mitigation level from the global optimum.

The results, so far, indicate the existence of an optimum protrusion length where the maximum mitigation is achieved for both RVR modes. Fourier spectra of the rotating and plunging components are displayed in figures 4 and 5 to discuss more details.

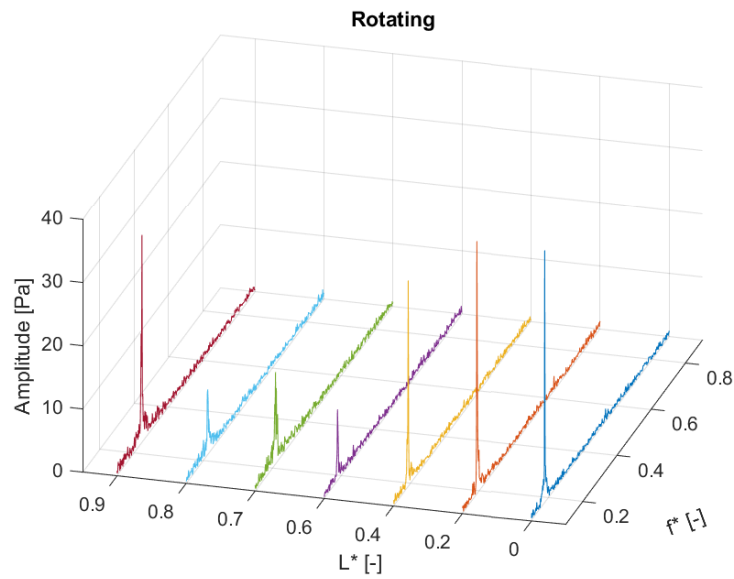


Figure 4. Spectra of the rotating mode amplitudes for different protrusion lengths.

The figures are drawn based on the pressure amplitudes in Pa, the dimensionless protrusion lengths, and frequency f^* that is defined as follows:

$$f^* = \frac{f}{f_n} \quad (4)$$

The overall trend for the amplitudes of the rotating component is similar to what has already been discussed. The mitigation becomes significant from $L^*=0.6$ and reaches the maximum level at $L^*=0.8$. This is followed by an increase of the amplitude at $L^*=0.9$. Moreover, no harmonics are observed in the spectra of the rotating component. However, the frequency of the RVR shifts with the increase of protrusion.

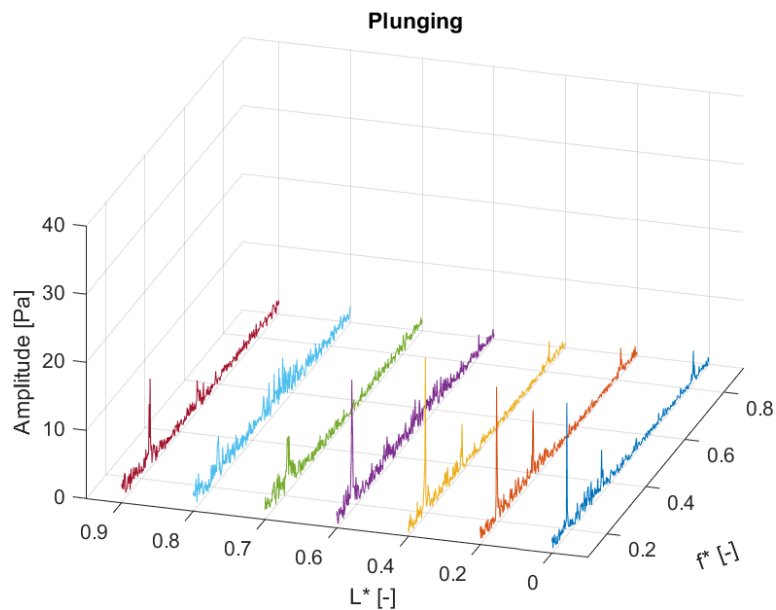


Figure 5. Spectra of the plunging mode amplitudes for different protrusion lengths.

The shifting of the RVR frequency with rod protrusion can also be observed in the spectra of the plunging mode. In addition, unlike the rotating mode, higher-order harmonics are present in the signal of the plunging mode. Specifically, the amplitude of the first harmonic of the plunging component starts to increase for small protrusion lengths. However, this harmonic decreases at $L^* = 0.6$ and completely disappears for $L^* = 0.7$ and $L^* = 0.8$. It then reappears for the protrusion length of $L^* = 0.9$. Another frequency can also be observed around $f^* = 0.8$. This frequency disappears after $L^* = 0.6$.

5. Discussion

Shorter protrusion lengths ($0 \leq L^* \leq 0.6$) are not found enough to affect the flow characteristics in the entire conduit. They only slightly increase the axial momentum in the center of the draft tube. This explains the small increase of the plunging mode (instead of any significant mitigation) as a global phenomenon until $L^* = 0.6$ [2]. The local nature of the rotating component means that to influence it effectively, a change of global flow characteristics is not necessarily needed. Thus, its mitigation can easily materialize even at shorter protrusion lengths only by swirl manipulation.

By inserting the rods into the swirling region, the tangential velocity of the flow decreases close to the walls. The conservation of the angular momentum dictates that the swirl of the flow in the center of the draft tube increases. The angular momentum can be defined as follows:

$$L = I\omega \quad (5)$$

where I is the angular inertia and ω is the rotational velocity that is defined as $\omega = 2\pi f$. If the angular inertia is defined as $I = mr^2$, then the angular momentum can be defined as:

$$L = 2\pi fmr^2 \quad (6)$$

By inserting the rods inside the swirling flow region, the area of swirling flow becomes constricted. Due to the reduction of the available radius for the swirl, RVR frequency increases to satisfy the conservation of angular momentum. Figure 6 shows RVR-related frequencies for each protrusion length.

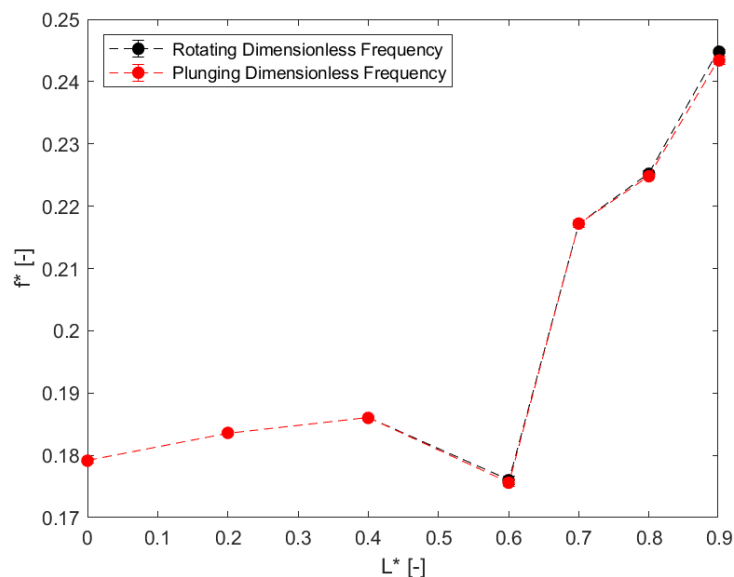


Figure 6. RVR dimensionless frequency at different protrusion lengths.

As can be seen, the frequency of the RVR increases for both modes with the increase of protrusion length. The only exception to this is $L^* = 0.6$ where the RVR frequency reaches its minimum, possibly due to the rods meeting the RVR as Shiraghaee et al. [18] previously explained, which falls in line

with the decrease of the RVR frequency. This length is where significant mitigation of the rotating component also happens in addition to what seems to be only the effects of swirl deceleration. The latter occurs due to the possible disruption of RVR structure and evolution by impacting the tip of the rods. Moreover, the significant mitigation of the plunging component which starts for $L^* > 0.6$ can be explained as a result of the effective blockage of axial flow structures. The effective mitigation of the rotating component happens for $0.6 \leq L^* \leq 0.8$ followed by a local increase of the rotating amplitude at $L^* = 0.9$. The former possibly happens due to the rods contacting with RVR from its outer surface at $L^* = 0.6$ until the interface of the stagnant region at $L^* = 0.8$. The continuous disruption of the RVR structure in contact with the tip of the rods causes its substantial mitigation. By increasing the protrusion to $L^* = 0.9$, the rods enter the stagnant region where the flow starts to adapt to the new boundary conditions causing the relative increase of the pressure pulsation amplitudes.

6. Conclusion

A series of experiments were conducted at Luleå University of Technology to study the effects of stationary rod protrusion on RVR mitigation. Different protrusion lengths were examined, and the results were analyzed based on time-resolved pressure data collected from two pressure sensors at the runner outlet. The results indicated significant mitigation of the RVR both in plunging and rotating components. For both components, there was an optimum protrusion length where the highest mitigation was achieved. The mitigation of the rotating component amplitude was attributed to the following:

- 1) Deceleration of the swirl at shorter protrusion lengths.
- 2) Interaction of the rod tips with the RVR structure.

The plunging component slightly increased at shorter protrusion lengths due to the increased axial momentum in the center of the draft tube for shorter protrusion lengths. Increasing the length of protrusion past the position of the RVR created a blockage of axial flow motion inside the draft tube leading to significant levels of plunging component mitigation.

The frequency of the RVR increased with the insertion of the rods. The conservation of angular momentum implies that the deceleration of the swirl near the wall should be compensated by increasing the angular momentum in the central region of the draft tube. Thus, the tangential flow velocity should increase in the mentioned region, manifested by the increase of RVR frequency. RVR frequency increased for all lengths except $L^* = 0.6$, where the rods probably meet the RVR.

The present paper aimed to investigate a novel method in mitigating draft tube pressure fluctuations induced by the presence of RVR at part-load operation. Through experiments, effects were quantified, the concept was examined, and the underlying physics was discussed. The results of the method proposed in this paper emphasize that the mitigation technique should be equipped with a closed-loop controller to assure efficient mitigation at different operating points. Possible future investigations can be dedicated to the assessment of the advantages as well as the shortcomings of the proposed method such as its impact on efficiency, its longevity, and its potential combination with other techniques. Also, the performance of the proposed method at other off-design conditions as well as other part-load operations is another issue that can be addressed in the future.

Acknowledgment:

This project has received funding from the European Union's Horizon 2020 research and innovation program under grant agreement No 814958.

References

- [1] Soltani Dehkharghani A, Engström F, Aidanpää J O and Cervantes M J 2020 *Sensors* **20** 7220 <https://doi.org/10.3390/s20247220>.
- [2] Amiri K, Mulu B, Raisee M and Cervantes M J 2016 *Journal of Hydraulic Research* **54** 56-73 <https://doi.org/10.1080/00221686.2015.1110626>.
- [3] Tănasă C, Bosioc A, Muntean S and Susan-Resiga R 2019 *Applied Sciences* **9** 4910 <https://doi.org/10.3390/app9224910>.
- [4] Amiri K, Cervantes M J and Mulu B 2015 *Journal of Hydraulic Research* **53** 452-465 <https://doi.org/10.1080/00221686.2015.1040085>.
- [5] Goyal R, Trivedi C, Gandhi B K, Cervantes M J and Dahlhaug O G 2016 *Sādhanā* **41** 1311-1320 <https://doi.org/10.1007/s12046-016-0556-x>.
- [6] Bosioc A I, Susan-Resiga R, Muntean S and Tanasa C 2012 *Journal of fluids engineering* **134** 8 <https://doi.org/10.1115/1.4007074>.
- [7] Goyal R, Cervantes M J and Gandhi B K 2017 *Journal of Fluids Engineering* **139** 041102 <https://doi.org/10.1115/1.4035224>.
- [8] Javadi A and Nilsson H 2017 *Engineering Applications of Computational Fluid Mechanics* **11** 30-41 <https://doi.org/10.1080/19942060.2016.1235515>.
- [9] Mohammadi M, Hajidavalloo E and Behbahani-Nejad M 2019 *Journal of Fluids Engineering*, vol 141 no 5 <https://doi.org/10.1115/1.4041565>.
- [10] Muntean S, Susan-Resiga R F, Campian V C, Dumbrava C and Cuzmos A 2014 In situ unsteady pressure measurements on the draft tube cone of the Francis turbine with air injection over an extended operating range *UPB Sci. Bull., Ser. D* **76** 173-180.
- [11] Nakanishi K and Ueda T 1964 Air supply into draft tube of Francis turbine *Fuji Electric Review* **10** 81-91.
- [12] Susan-Resiga R, Vu T C, Muntean S, Ciocan G D and Nennemann B 2006 Jet control of the draft tube vortex rope in Francis turbines at partial discharge *23rd IAHR Symp. Conf. Yokohama* 67-80.
- [13] Vilberg I K, Kjeldsen M, Escaler X, Ekanger J and Nielsen T 2019 Influence of draft tube water injection system on cavitation behaviour in a full-scale Francis turbine with visual access *IOP Conf. Series: Earth and Environmental Science Kyoto* **240** 022015 [doi:10.1088/1755-1315/240/2/022015](https://doi.org/10.1088/1755-1315/240/2/022015).
- [14] Holmström H, Sundström J and Cervantes M 2021 Vortex rope mitigation with azimuthal perturbations: A numerical study *IOP Conf. Series: Earth and Environmental Science Lausanne* **774** 012144 [doi:10.1088/1755-1315/774/1/012144](https://doi.org/10.1088/1755-1315/774/1/012144).
- [15] Nishi M, Wang X, Yoshida K, Takahashi T and Tsukamoto T 1996 *Hydraulic machinery and cavitation* 905-914 https://doi.org/10.1007/978-94-010-9385-9_92.
- [16] Zhou X, Wu H G and Shi C Z 2019 Numerical and experimental investigation of the effect of baffles on flow instabilities in a Francis turbine draft tube under partial load conditions *Advances in Mechanical Engineering* **11** 1687814018824468 <https://doi.org/10.1177/1687814018824468>.
- [17] Tănasă C, Bosioc A, Muntean S and Susan-Resiga R 2015 Experimental and Numerical Assessment of the Velocity Profiles Using a Passive Method for Swirling Flow Control *Proc. of the 6th IAHR Int. Meeting of the Workgroup on Cavitation and Dynamic Problems in Hydraulic Machinery and Systems (IAHRWG2015) Ljubljana* 9-11.
- [18] Shiraghaee S, Sundström J, Raisee M and Cervantes M J 2021 Mitigation of Draft Tube Pressure Pulsations by Radial Protrusion of Solid Bodies into the Flow Field: An Experimental Investigation *IOP Conf. Series: Earth and Environmental Science Lausanne* **774** 012004 [doi:10.1088/1755-1315/774/1/012004](https://doi.org/10.1088/1755-1315/774/1/012004).

- [19] Joy J, Raisee M and Cervantes M J 2021 Study of Flow Characteristics inside Francis Turbine Draft Tube with Adjustable Guide Vanes *IOP Conf. Series: Earth and Environmental Science* Lausanne **774** 012018 doi:10.1088/1755-1315/774/1/012018.
- [20] Amiri K, Mulu B, Raisee M and Cervantes M 2015 Velocity measurements within an elbow type draft tube of a Kaplan turbine *10th Pacific symp. on flow visualization and image processing* Naples.
- [21] Jonsson P, Mulu B and Cervantes M 2012 *Applied Energy* **94** 71-83, 2012 <https://doi.org/10.1016/j.apenergy.2012.01.032>.
- [22] Soltani Dehkharghani A, Engström F, Aidanpää J O and Cervantes M J 2020 *Journal of Fluids Engineering* **142** <https://doi.org/10.1115/1.4047793>.